



1 **A case for a pragmatic oxygen-based approach to quantifying 2 the biological contribution to the marine carbon sink.**

3 Wolfgang Koeve¹, Ivy Frenger¹

4 ¹Biogeochemical Modelling, GEOMAR Helmholtz Centre for Ocean Research Kiel, Wischhofstraße 1-3, 24148
5 Kiel, Germany

6 Correspondence to: Wolfgang Koeve (wkoeve@geomar.de) and Ivy Frenger (ifrenger@geomar.de)

7 **Abstract.** AOU, the ‘apparent oxygen utilization’, is a widely used concept in ocean biogeochemistry to assess
8 and interpret ocean deoxygenation and changes of the marine carbon cycle. It provides an estimate of oxygen (O_2)
9 used and dissolved inorganic carbon (DIC) released during organic matter degradation in the ocean interior. AOU
10 is calculated from observations of temperature, salinity and O_2 . This calculation relies on the assumption that
11 surface water O_2 is in equilibrium with the atmosphere when water masses form and sink into the interior ocean.
12 Using specifically designed idealized model tracers, we here provide an evaluation of the reliability and
13 uncertainty of this approach. Global AOU reliably estimates total oxygen debt, defined as the sum of ‘true’ oxygen
14 utilization (TOU) since last contact with the atmosphere and biotic oxygen disequilibrium ($O_2^{dis,bio}$). AOU and
15 TOU + $O_2^{dis,bio}$ agree to within about 10%, both for the preindustrial state estimate and the transient climate change
16 situations explored. Taking differences of the biotic components of the O_2 and DIC disequilibrium ($DIC^{dis,bio}$) into
17 account, we find that, for the pre-industrial state estimate, the carbon equivalent of AOU is an about 15%
18 underestimate of the sum of DIC^{remin} and $DIC^{dis,bio}$. For the climate change transient we find that ΔAOU
19 underestimates our estimates of the disequilibrium corrected change in C^{soft} ($DIC^{remin} + DIC^{dis,bio,COU^*,BGC^*}$) by 25%
20 . In summary, we suggest that AOU in particular can be used to assess causes of ocean deoxygenation, and is a
21 very useful proxy for changes of storage of biologically processed carbon under various climate change scenarios.

22 **1 Introduction**

23 To gain insights into marine biogeochemical cycling and the marine carbon sink, “apparent” oxygen utilization
24 (AOU) is a powerful quantity. It describes the deviation of the observed O_2 concentration (O_2^{obs}) from the
25 saturation state (O_2^{sat}), given the local temperature and salinity. The concept behind this is that temperature and
26 salinity properties are conserved in the ocean interior while O_2 is not. Thus local temperature and salinity provide
27 information about the initial, apparently saturated, O_2 concentrations of waters journeying through the ocean
28 interior. Being one of the oldest concepts in ocean biogeochemistry, dating back to at least the 1930 to 1940
29 (Redfield, 1934, 1942), AOU provides in particular an estimate of the interior ocean O_2 debt deriving from the O_2
30 consumed during organic matter degradation. In deoxygenation research, it has been used to distinguish between
31 marine O_2 loss due to surface ocean warming and reduced physical O_2 solubility from that of changes in biotic O_2
32 usage in the interior ocean (Emerson et al., 2001; Keeling et al., 2010; Takano et al., 2018; Ito et al., 2017;
33 Schmidtko et al. 2017).

34

35 More recently, by conversion of O_2 debt to respired carbon, AOU has further been used to quantify the contribution
36 of the biological ‘soft tissue’ pump to dissolved inorganic carbon stored in the interior ocean (Ogura et al., 1970;



37 Doval and Hansell, 2000; Gruber et al., 1996; Sarmiento and Gruber, 2006; Schwinger and Tjiputra, 2018; Wilson
38 et al., 2022). The term soft tissue pump, one of two biological carbon pumps (Volk and Hoffert, 1985), comprises
39 the biological production of organic matter, its transport into the interior ocean and its degradation to dissolved
40 inorganic carbon there. So far, under positive CO₂-emissions, the soft tissue pump has been estimated to contribute
41 little to the marine carbon sink, which is defined as the excess marine carbon since preindustrial times (Koeve et
42 al., 2020; Wilson et al., 2022; Frenger et al., 2024). However, it has been projected that dissolved inorganic carbon
43 (DIC) attributable to the soft tissue pump may become an important, even the dominant, sink after temperature
44 overshoot (Koeve et al., 2024). A pragmatic approach - that the AOU concept provides - is needed to quantify this
45 contribution to the marine carbon sink, both in models and future ocean observations.

46

47 Despite its value for interpreting ocean changes of oxygen and carbon, and in parallel to the wide usage, a
48 canonical criticism of the AOU concept has been that it is prone to significant uncertainties (e.g. Ito et al., 2004;
49 Sarmiento & Gruber, 2006; Duteil et al., 2013; Wolf et al., 2018; Mackay and Watson, 2021; Carter et al., 2021).
50 The major critique is the assumption of perfect equilibration of surface ocean O₂ with the atmosphere that is built
51 into the computation of AOU (sidenote: here defined as a negative property because consumption reduces O₂,
52 AOU = O₂ - O₂^{sat}, where generally O₂ < O₂^{sat}). The assumption of perfect equilibration is unrealistic, for example
53 when gas exchange is slowed down due to sea ice cover or when a large atmosphere-ocean O₂-difference is created
54 e.g., when waters with a large O₂ debt upwell into surface water (e.g. Gordon and Huber, 1990; Körtzinger et al.,
55 2004). Under such conditions surface O₂ can remain undersaturated as waters subduct into the ocean interior
56 (Keeling et al., 2010; Ito et al., 2004; Duteil et al., 2013). Beyond the assumption of perfect surface O₂ saturation,
57 other points of critique are that mixing effects and subsurface warming affect local temperature or salinity. This
58 can contribute to uncertainties in the AOU estimate, by introducing biases into O₂^{sat} as an estimate of surface
59 water O₂ characteristics (Dietze and Oschlies, 2005). Estimating, based on AOU, in an additional step, the fraction
60 of DIC which can be attributed to the soft tissue pump (Volk and Hoffert, 1985) comes also with uncertainties,
61 stemming from the carbon-to-oxygen demand of organic matter degradation (R_{CO}) (Körtzinger et al., 2001;
62 Tanioka and Matsumoto, 2020) and differences in O₂ and CO₂ disequilibria (see below).

63

64 Despite these caveats of the AOU concept, we argue in this work for its high interpretational value based on a
65 reevaluation of the concept for (a) quantifications of the integrated ocean biotic O₂ utilization and (b)
66 quantifications of the contribution of the biological soft tissue pump to marine carbon storage. Using output from
67 an Earth system model, we compare AOU-based estimates against estimates using several established approaches
68 to directly assess (a) and (b) in models based on idealised model tracers. We apply, for example, a tracer of 'true'
69 oxygen utilization, TOU (Ito et al. 2004; see Methods for details) as well as additional model tracers, such as
70 properties of waters as they subduct to the ocean interior ("preformed" properties, e.g. preformed phosphate,
71 PO₄^{pre}). We also apply idealized model tracers and experimental protocols which allow us to explicitly quantify
72 effects of incomplete air-sea equilibration of oxygen and carbon. We define the usefulness of the AOU
73 approximation for the preindustrial steady state, and decadal to centennial climate change projections.

74



75 **2 Methods**

76 We used a modified version of the UVic Earth System Model of intermediate complexity 2.9 (Weaver et al. 2001;
77 Eby et al. 2013), which we ran in ocean-atmosphere-sea-ice configuration (Koeve et al., 2020). The ocean
78 biogeochemistry used in this model was based on a NPZD model, with phosphate and nitrate as prognostic
79 nutrients and iron limitation prescribed by an iron concentration mask (Keller et al., 2012). The model simulated
80 diazotrophs and ordinary phytoplankton, one zooplankton and one detritus pool. It applied fixed elemental ratios
81 (C:N:P:O₂) for organic matter cycling and the interactions with prognostic O₂, DIC, and alkalinity tracers.
82 Degradation of organic matter was temperature sensitive. For more details on model equations and evaluation
83 against observations see Keller et al. 2012.

84

85 We implemented idealized model tracers in order to distinguish contributions from different processes on O₂,
86 DIC, and phosphate (PO₄) (Ito et al., 2004; Ito and Follows, 2005; Bernardello et al., 2014; Koeve et al., 2020;
87 Koeve et al., 2024). Preformed properties (DIC^{pre}, O₂^{pre}, PO₄^{pre}) represent the fractions of DIC, O₂, and PO₄ which
88 reflects surface water characteristics transported and mixed into the ocean interior, and behave conservatively
89 within the ocean: At the surface DIC^{pre} (O₂^{pre}, PO₄^{pre}) were set to the values of DIC (O₂, PO₄), in the interior ocean
90 (z > 50m) they had no biogeochemical sources or sinks. Remineralized properties (DIC^{remin}, TOU, PO₄^{remin})
91 represented the impact of organic matter degradation on O₂, DIC and PO₄ in the interior ocean. Below the surface
92 layer (i.e. below z = 50m in this model) TOU and DIC^{remin} (PO₄^{remin}) were subject to source-minus-sink terms
93 associated with organic matter degradation (and production). When organic matter is degraded by oxic
94 metabolism, O₂ is used (the value of TOU becomes more negative) and DIC (PO₄) is released (DIC^{remin} and
95 PO₄^{remin} increase). In the surface layer TOU, DIC^{remin}, and PO₄^{remin} are set to zero at any time step during model
96 runtime. Mass balance applies:

97

$$98 \quad O_2 = O_2^{\text{pre}} + \text{TOU} \quad (1)$$

$$99 \quad PO_4 = PO_4^{\text{pre}} + PO_4^{\text{remin}} \quad (2)$$

$$100 \quad DIC = DIC^{\text{pre}} + DIC^{\text{remin}} + DIC^{\text{ca}}, \quad (3)$$

101

102 with DIC^{ca} representing DIC stemming from CaCO₃ dissolution in the interior ocean. Idealised tracers have no
103 explicit gas exchange, while bulk tracers (O₂, DIC) have.

104

105 As a counterpart of biotically influenced O₂, we further simulate abiotic O₂ (O₂^{abiot}, Oschlies et al., 2019). This
106 tracer has no biotic sinks or source but gas exchange with the atmosphere. A tracer of saturated DIC (DIC^{sat}) is
107 computed in the model surface layer at runtime from surface alkalinity, temperature, salinity, PO₄ and the
108 contemporary atmospheric pCO₂. Within the interior ocean DIC^{sat} is a passive tracer, i.e. has no sources or sinks.
109 All idealized model tracers were transported according to the model physics and could be (further) modified due
110 to mixing of water masses. In the following we reiterate how the idealized tracers relate to infer information about
111 incomplete surface equilibration due to biotic and ‘physical’ effects, and how those relate to AOU.

112

113 The biological contribution to the O₂ disequilibrium is defined as:

114



115 $O_2^{\text{dis,bio}} = O_2^{\text{pre}} - O_2^{\text{abiot}}$ (4)

116

117 Since O_2^{abiot} has no biological sources-or-sinks, it represents the physical conditions at water mass formation,
118 including deviations from equilibration, i.e. $O_2^{\text{abiot}} = O_2^{\text{sat}} + O_2^{\text{dis,phys}}$. The latter, by reordering, provides info about
119 the physical contribution to the O_2 disequilibrium, $O_2^{\text{dis,phys}} = O_2^{\text{abiot}} - O_2^{\text{sat}}$. The superscript ‘phys’ denotes that the
120 inherent driver of this disequilibrium component is either warming or cooling of the surface water or a change in
121 surface salinity, with thermal effects dominating $O_2^{\text{dis,phys}}$ - that is physical processes. Note further, that processes
122 that affect the speed of gas exchange, like wind speed, sea state, sea ice cover, or properties of the surface
123 microlayer (Wanninkhof, 2014; Salter et al., 2011; Gutiérrez-Loza et al., 2022) affect $O_2^{\text{dis,bio}}$ and $O_2^{\text{dis,phys}}$ alike.

124

125 To reflect the meaning of equ. (4), consider the entrainment of water rich in O_2 -debt (i.e. TOU) into the surface
126 layer before equilibration. (a) The observed surface O_2 concentration decreases. (b) According to our tracer
127 definitions TOU is set to zero at the surface and O_2^{pre} is set equal to O_2 , i.e. decreases as well. (c) Entrainment
128 would affect O_2^{abiot} only, if temperature or salinity of the entrained water differ from those of the surface water
129 (i.e. $O_2^{\text{dis,phys}}$). The entrained TOU-signal hence ‘hides’ in the modified O_2^{pre} , but does not affect O_2^{abiot} . The biotic
130 O_2 -disequilibrium is hence given by the difference of O_2^{pre} and O_2^{abiot} (equation 4). Allowing time for
131 equilibration, i.e. flux of O_2 into the ocean for the given example, (and assuming no change in surface temperature
132 and salinity, no biological production or further entrainment), O_2 and O_2^{pre} increase in lockstep, O_2^{abiot} stays
133 constant and $O_2^{\text{dis,bio}}$ diminishes. Similarly, biological production in the surface layer will affect O_2 and O_2^{pre} , but
134 not O_2^{abiot} , and hence can give rise to a (positive) $O_2^{\text{dis,bio}}$.

135

136 The apparent oxygen utilization is quantified as

137

138 $AOU = O_2^{\text{obs}} - O_2^{\text{sat}}$ (5)

139

140 with the observed O_2 concentrations, O_2^{obs} and the O_2 saturation, O_2^{sat} , computed from the model’s potential
141 temperature and salinity (Garcia and Gordon, 1992). Note that we use a definition of AOU, which differs from
142 the usually used one (i.e. $AOU = O_2^{\text{sat}} - O_2^{\text{obs}}$, e.g. Sarmiento and Gruber, 2006), intentionally, by the sign. This
143 is done for consistency with the sign of TOU and the fact that AOU and TOU reflect an O_2 debt, i.e. O_2 missing
144 in the ocean compared with O_2^{sat} . That is, throughout this paper, we use O_2^{sat} as the reference point in all equations.
145 AOU can be rewritten as accumulated sources-minus-sinks (TOU) since last contact with the atmosphere plus
146 surface-set disequilibrium conditions, $O_2^{\text{dis,bio}}$ and $O_2^{\text{dis,phys}}$.

147

148 $AOU = TOU + O_2^{\text{dis,bio}} + O_2^{\text{dis,phys}}$ (6)

149

150 We note that the computation of O_2^{sat} from temperature and salinity which have been affected by mixing in the
151 interior ocean or by sub-surface warming can cause a low bias (Dietze and Oschlies, 2005). That is, computing
152 O_2^{sat} can give a smaller value compared to O_2^{sat} from an explicit O_2^{sat} tracer which is computed at the surface given
153 surface temperature and salinity and mixed passively in the interior ocean. This effect however, is, globally, much
154 smaller compared to the disequilibria evaluated in this study (Fig. S9) and ignored henceforth.



155

156 For carbon, we will compare the carbon equivalent of AOU against the sum of an explicit tracer of remineralized
157 DIC, DIC^{remin} and an estimate of the biotic contribution to the DIC disequilibrium, $DIC^{dis,bio}$. The carbon equivalent
158 of AOU (the ‘AOU approximation’) is computed by multiplying AOU with the O_2 demand of organic matter
159 remineralisation applied in the model, $R_{C,O_2} = -0.66$ mol:mol. In the real ocean (or in models with variable
160 stoichiometry) this conversion is complicated by uncertainties and variability of R_{C,O_2} . Fortunately, this turns out
161 to be a comparatively minor uncertainty, given the relative constancy of this ratio (Körtzinger et al., 2001; Tanioka
162 and Matsumoto, 2020).

163

164 To derive $DIC^{dis,bio}$, we proceed as follows: We first compute the total DIC disequilibrium from the difference of
165 idealised model tracers DIC^{pre} and DIC^{sat} .

166

$$167 DIC^{dis} = DIC^{pre} - DIC^{sat} \quad (7)$$

168

169 Attributing DIC^{dis} to physical versus biological effects is not straightforward as there is no meaningful definition
170 of an abiotic DIC tracer in an Earth system model where atmospheric CO_2 is affected by ocean biology. For O_2
171 the atmospheric reservoir is large and changes in marine oxygen can be neglected when computing the
172 atmospheric oxygen boundary condition of the ocean; this is very different for carbon - also since carbon affects
173 the climate. Computation of the biotic component of DIC^{dis} , $DIC^{dis,bio}$, is thus based on additional model
174 experiments carried out with two variants of our default model, one with all marine carbon pumps turned on
175 (allPumps) and one in which the impact of biological carbon pumps on alkalinity and DIC is disabled
176 (noBioPumps). Both model variants are run into steady state, conserving the atmosphere+ocean total CO_2
177 inventory (mass conserving approach). Pre-industrial state estimates presented in this work (Fig. 1b; Tab. S1) are
178 based on this steady state model output.

179

180 Following Khatiwala et al. (2019), $DIC^{dis,bio}$ is computed as

181

$$182 DIC^{dis,bio} = DIC^{dis,allPumps} - DIC^{dis,noBioPumps} \quad (8)$$

183

184 Starting from the respective steady states, we perform the default transient model experiments by applying CO_2 -
185 emissions following the bell shape 1000 Pg C ZECmp (Zero Emission Commitment Model Intercomparison
186 Project) protocol (Jones et al., 2019). In this protocol, CO_2 -emissions are restricted to the first 100 years, with net-
187 zero CO_2 emissions thereafter (Fig. S3a). We integrated the model for a total of 800 years. This experiment is
188 performed with the allPumps and the noBioPumps model variants in two setups. In the default setup (COU*) the
189 model is fully coupled, i.e. CO_2 -emissions cause global warming and climate and circulation change. In the second
190 setup (BGC*) the climate is kept constant at the preindustrial state.

191

192 Applying equation 8 to output from the COU* and BGC* experiment, we derive the climate change component
193 of $DIC^{dis,bio}$ from the respective difference of the fully coupled and the BGC-only coupled model variants.

194



195 $DIC_{dis,bio,COU^*-BGC^*} = DIC_{dis,bio,COU^*} - DIC_{dis,bio,BGC^*}$ (9)

196

197 Our approach of BGC-only and fully coupled model differs from the standardized approach widely used in
198 climate-feedback research (e.g. Arora et al., 2020) by the usage of CO₂-emissions instead of a prescribed pCO₂^{atm}
199 trajectory in the allPumps experiment (hence COU* and BGC*). In the noBioPumps COU* experiment, we
200 prescribe the climate change trajectory from the allPumps experiment. This approach is chosen in order to derive
201 the climate change component of the biological disequilibrium of the fully coupled model experiment of the
202 allPumps model variant.

203

204 We further conducted a series of sensitivity experiments with versions of the default model in which we either
205 change the vertical background diffusivity, or the rate with which the sinking speed increases over depth, always
206 keeping all other model parameters like in the default model. Changing the vertical background diffusivity causes
207 changes in the overturning circulation (Duteil and Oschlies, 2011; Fig. S2b), which, with otherwise constant
208 physical and biogeochemical parameters, causes a considerable range of C^{remin} to establish during the model
209 spinup (Frenger et al., 2024; Fig. S2b). In experiments with modified sinking speed increase over depth, we find
210 larger global C^{soft} in experiments with deeper organic matter penetration and vice versa (Frenger et al., 2024; Fig.
211 S2a). Over all experiments, the AOU spread ranges from -167 to -217 Pmol O₂. The AOU inventory of the World
212 Ocean Atlas (2013, Garcia et al., 2014), regridded to the UVic model grid, is -207 Pmol O₂. Model variants are
213 explored with respect to the steady state relationship of AOU vs. TOU+O₂^{dis,bio} (Fig. 3a) and how these properties
214 respond to a high CO₂-emissions (RCP 8.5) climate change forcing (Fig. 3b).

215

216 **3 Results and Discussion**

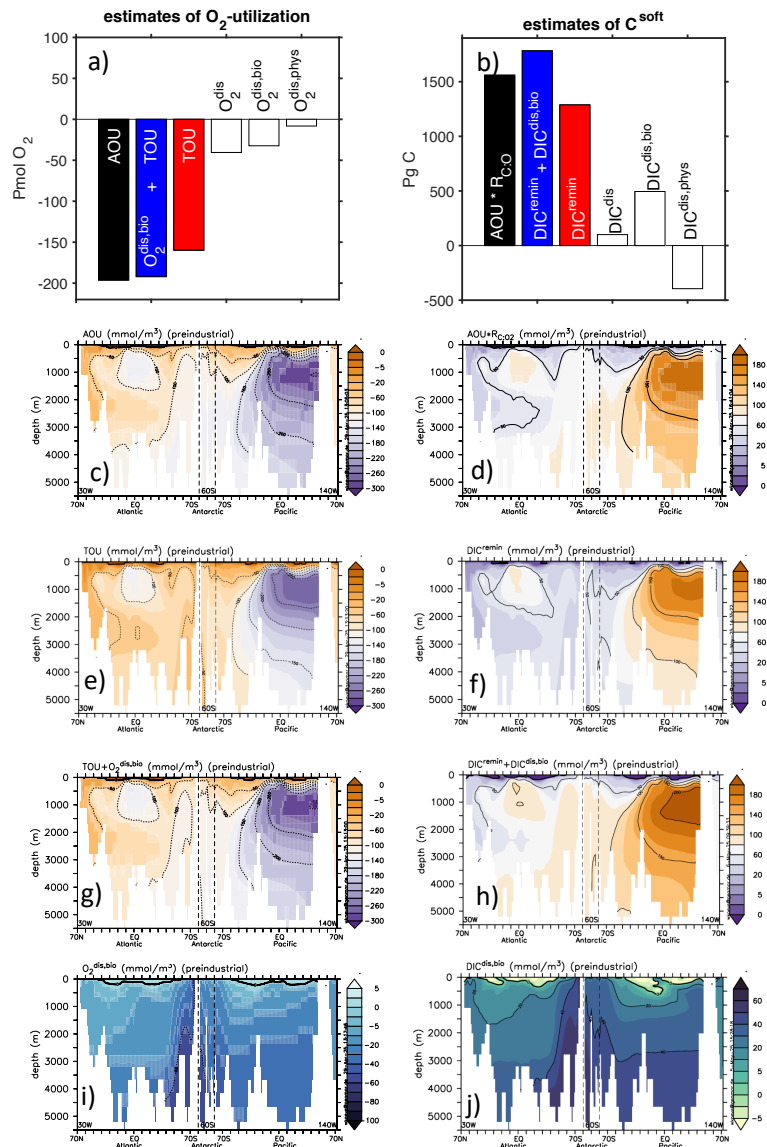
217 **3.1 AOU as an estimate of biotic oxygen utilization**

218 The preindustrial state of our default model configuration (Keller et al., 2012) confirms earlier publications (Ito
219 et al., 2004, Duteil et al., 2013), namely that the global integral of AOU (-196.5 Pmol O₂) is larger in magnitude
220 than the global integral of TOU (-160 Pmol O₂) (Fig. 1a, c, e). This is due to systematic O₂ undersaturation of
221 surface waters as they subduct to the ocean interior, causing O₂^{sat} to be a too large estimate for surface ocean O₂
222 conditions (O₂^{sat} > O₂^{pre}; Fig. S1 and see Methods for technical tracer definitions). Globally, most of this
223 difference, about 80%, is explained - rather than by the, primarily, thermal effect of solubility increase due to
224 cooling - by upwelling of undersaturated waters that carry the O₂ debt stemming from organic matter

225

226

227



228

229 **Fig. 1: Preindustrial steady state estimate of estimates of oxygen utilization and soft tissue pump carbon storage from**
 230 **the default UVic model variant. Global estimates of O_2 -utilization (a, Pmol O_2) and soft tissue pump carbon storage (b,**
 231 **Pg C). Distribution of O_2 -utilization estimates (c, e, g) and C^{remin} estimates (d, f, h) along sections through the Atlantic**
 232 **(30°W, from North to South), the Southern Ocean (60°S), and the Pacific Ocean (140°W, from South to North), showing**
 233 **apparent oxygen utilization, AOU (c, $\text{mmol } O_2 / m^3$), the sum of TOU and the biotic contribution to the O_2 disequilibrium ($O_2^{dis,biol}$,**
 234 **TOU+ $O_2^{dis,biol}$ (g, $\text{mmol } O_2 / m^3$), the carbon equivalent of AOU ($AOU \cdot R_{CO}$) (d, $\text{mmol } C / m^3$), remineralised DIC,**
 235 **DIC^{remin} (f, $\text{mmol } C / m^3$), the sum of DIC^{remin} and the biotic contribution to the DIC disequilibrium, $DIC^{dis,biol}$ (DIC^{remin}**
 236 **+ $DIC^{dis,biol}$) (h, $\text{mmol } C / m^3$). Panels (i) and (j) show Atlantic-SO-Pacific Ocean transects of $O_2^{dis,biol}$ ($\text{mmol } O_2 / m^3$)**
 237 **and $DIC^{dis,biol}$ ($\text{mmol } C / m^3$), respectively. For tracer definitions and details on computation see the Methods.**



239 degradation in the interior ocean (Fig. 1a, Fig. S2). We refer to this ‘biological’ contribution to the total O₂
240 disequilibrium as O₂^{dis,bio} (Fig. 1a, i) and assess it from the difference of our idealised tracers of preformed O₂
241 (O₂^{pre}) and ‘abiotic’ O₂ that is unaffected by biology, O₂^{abiotic} (see Methods for technical tracer definitions,
242 rationale and Eq. 4). Under a stable, preindustrial climate, O₂^{dis,bio} is largest in magnitude in waters ventilated in
243 the Southern Ocean (Fig. 1i), consistent with the finding that sea ice cover limits complete O₂ equilibration, in
244 particular in regions where waters with a large O₂ debt from organic matter degradation return to the surface (Ito
245 et al., 2004). The fact that AOU is larger than TOU (Fig. 1a, c, e) in magnitude indicates that, while TOU is an
246 appropriate measure of the accumulated O₂ utilization of interior ocean waters *since last contact with the*
247 *atmosphere*, it is in fact not a good measure of the total accumulated O₂ debt associated with the degradation of
248 organic matter in the interior ocean. AOU, in turn, adds the information of the effect of biologically induced
249 undersaturation of waters at the beginning of their next journey through the interior ocean. AOU equals
250 TOU+O₂^{dis,bio} (Fig. 1c, g; globally with only 2% uncertainty, Fig. 1a) in our default model setup which had been
251 tuned to represent observations of O₂ and macronutrients (Keller et al., 2012). It hence provides a very reliable
252 global state estimate of the *total* biological effect on O₂, and we will discuss in the following to which extent AOU
253 agrees with TOU+O₂^{dis,bio} in a changing climate and for other variants of our model.

254

255 Confronted with an idealised climate change scenario (Fig. S3; Methods), the Earth system model shows that
256 AOU consistently increases in magnitude, and that the change in AOU roughly corresponds to the change in
257 TOU+ O₂^{dis,bio}. While the magnitude of Δ AOU is considerably smaller than the magnitude of Δ TOU (Fig. 2a),
258 e.g. by about 30% in year 100, when emissions decrease to net-zero (Fig. S3a), the difference of Δ AOU and
259 Δ (TOU+ O₂^{dis,bio}) is small. This is so since most, about 2/3, of the former difference is explained by changes in
260 O₂^{dis,bio}. The loss in sea ice observed in both high latitudes in particular during the initial 100 year time period of
261 net-positive CO₂ emissions and global warming (see Fig. S3c,d) allows for a more complete O₂ equilibration
262 compared with the preindustrial state (Fig. S4). Globally, the change in AOU underestimates the combined change
263 in TOU+O₂^{dis,bio} by less than 10% until year 100 (Fig. 2a). During the rest of the experiment the relative difference
264 between Δ AOU and Δ TOU+ Δ O₂^{dis,bio} stays in the range of 10 to 13% (Fig. S5), despite diverging Δ AOU and
265 Δ TOU (Fig. 2a), since the magnitude of O₂^{dis,bio} continues to decrease - with an almost stable climate under net-
266 zero CO₂-emissions, sea ice does not return and old waters ventilated at high latitudes gradually adjust (Fig. S3d).

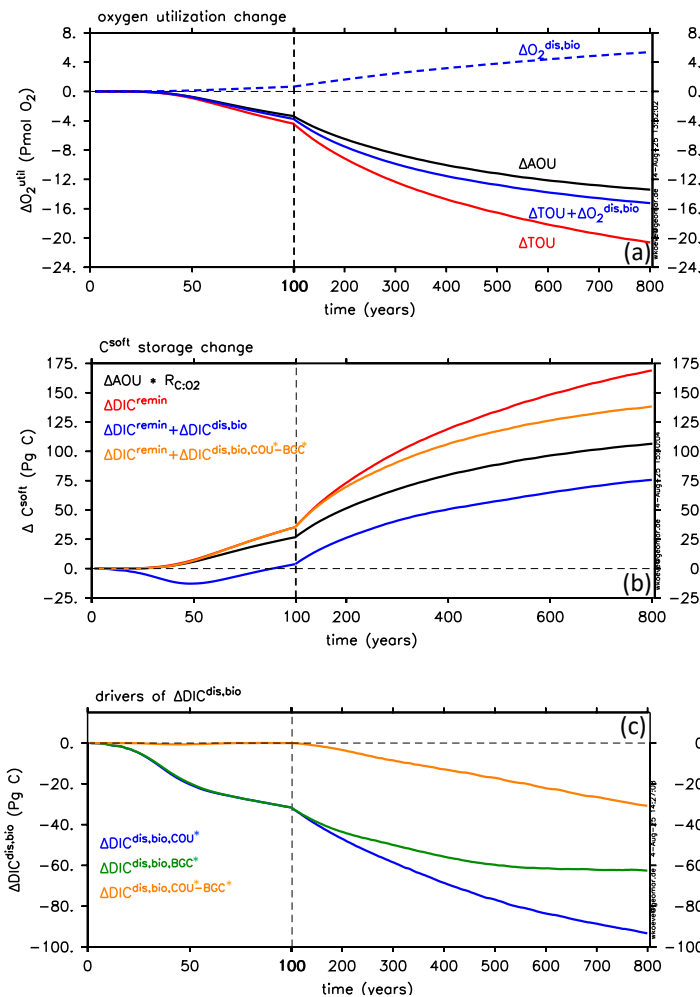
267

268 We test the robustness of our findings from a suite of additional model experiments carried out with different
269 variants of the default UVic model (Frenger et al., 2024). We explore variants which are characterized by smaller
270 or larger mixing and Atlantic meridional overturning circulation (AMOC) and identical parameterization of ocean
271 biogeochemistry, and variants with the default mixing and AMOC but modified particle flux attenuation, i.e.
272 shallower or deeper remineralization of organic matter (for details, see Methods, Sensitivity experiments).
273 Running these models into their own climate and biogeochemical steady states allows us to compare the
274 preindustrial globally integrated AOU with the respective sum of TOU and O₂^{dis,bio} (Fig. 3a). The majority of
275 model variants show a small deviation of AOU from TOU+O₂^{dis,bio}, consistent with our default model.

276

277

278



279

280 **Fig. 2: Temporal development of global integral estimates of oxygen utilization, soft tissue pump carbon storage and**
 281 **drivers of DIC disequilibria under a changing climate. Globally integrated changes in O₂-utilization (a, Pmol O₂), soft**
 282 **tissue pump carbon storage (b, Pg C) and biotic DIC disequilibria (c, Pg C) from the default model variant are shown**
 283 **with split x-axes, with higher resolution of the time period with bell shaped CO₂ emissions following the 1000 Pg**
 284 **ZECmp scenario, compared with the 700 year long period with net-zero emissions. Estimates of O₂-utilization (a):**
 285 **ΔAOU (black solid), ΔTOU (red solid), ΔTOU+ΔO₂^{dis,bio} (blue solid), ΔO₂^{dis,bio} (blue dashed). C^{soft} change estimates (b):**
 286 **carbon equivalent of AOU changes (ΔAOU* R_{C:O₂}, black solid), change in remineralized DIC accumulated since last**
 287 **contact with the atmosphere (ΔDIC^{remin}, red solid; see Fig. S7 for a comparison with additional tracer based estimates),**
 288 **sum of ΔDIC^{remin} and total ΔDIC^{dis,bio} (blue solid), and sum of ΔDIC^{remin} and the climate change component of**
 289 **ΔDIC^{dis,bio}, ΔDIC^{dis,bio, COU*-BGC*} (orange solid). Drivers of the biotic component of the DIC disequilibrium, ΔDIC^{dis,bio}**
 290 **(c): experiment COU* - effect of changing atmospheric pCO₂ boundary condition and climate change (blue solid),**
 291 **experiment BGC* - effect of changing atmospheric pCO₂ boundary condition only (green dashed), difference COU* -**
 292 **BGC* - effect of changing climate only (orange solid). Compare Fig. S3 for CO₂-emissions and various climate change**
 293 **indicators of this experiment.**



294 Confronting the model variants with a high-end CO₂-emissions scenario (Frenger et al., 2024; see Methods), we
295 consistently find for all model variants that ΔAOU underestimates the total change of the O₂ debt due to organic
296 matter degradation ($\Delta\text{TOU} + \Delta\text{O}_2^{\text{dis,bio}}$), as in the default model, by about 10% or less (Fig. 3b). The underestimate
297 is rather small and robust in that it shows no dependence on the initial (preindustrial) mixing and overturning or
298 the imposed variations of particle flux attenuation. That is $\Delta\text{AOU} \approx \Delta\text{TOU} + \Delta\text{O}_2^{\text{dis,bio}}$ is generally valid. Finally,
299 we confront our default model with a suite of CO₂ reversibility experiments (Fig. 3c), i.e. experiments which show
300 various degrees of negative emissions after the models had been forced by a 1% pCO₂ increase per year until
301 pCO₂-doubling (Koeve et al., 2024). This causes the models to go through sequences of initial warming and
302 circulation slow down and subsequent cooling and recovery of circulation (Fig. S6). Despite these complex
303 changes of ocean circulation, O₂ equilibration conditions and also biological changes (not shown), ΔAOU is
304 robustly able to estimate $\Delta\text{TOU} + \Delta\text{O}_2^{\text{dis,bio}}$ to within about 10% uncertainty (Fig. 3c).

305

306 We conclude that globally integrated AOUs provides a very reliable estimate of the total O₂ debt from organic
307 matter degradation, which, based on our additional tracers, we describe by the sum of TOU + O₂^{dis,bio}. This is the
308 case for the state estimate and the transient situations explored, with deviations of around 10% (or less). We
309 suggest AOUs hence to be a suitable metric to quantify changes in biotic O₂ usage in the interior ocean in the
310 framework of ocean deoxygenation research.

311

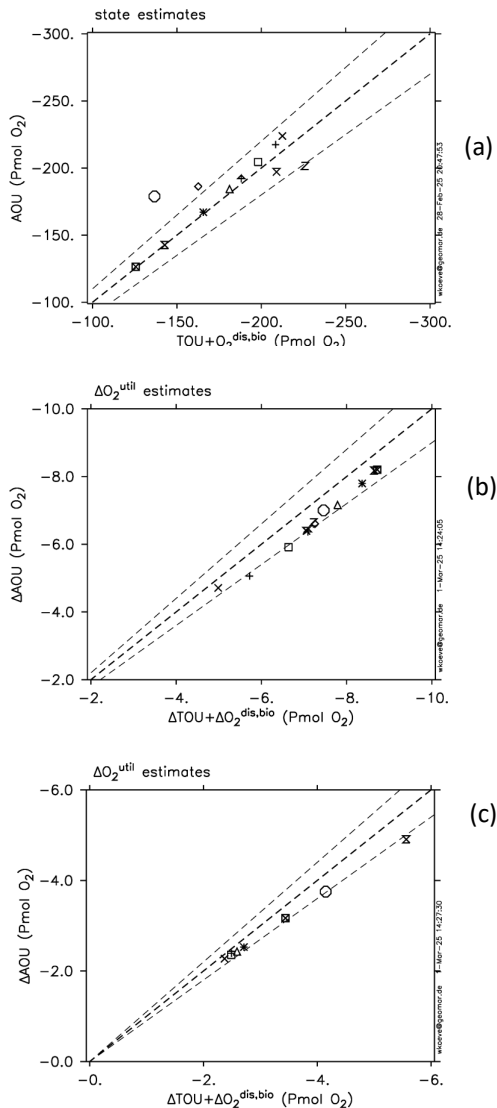
312 **3.2 AOUs as estimate of soft tissue pump carbon**

313 In this section we explore whether AOUs, beyond attributing changes of oxygen to biology, can also be used to
314 estimate changes of carbon due to biology. We refer to the fraction in DIC which can be attributed to the soft
315 tissue pump as ‘soft tissue pump carbon’, C^{soft}. In analogy to our findings above, we consider C^{soft} to be a
316 composite of (a) C^{soft} accumulated since last contact with the atmosphere and (b) a recirculated biotic component
317 of the carbon disequilibrium. We trace the former by an idealised model tracer, DIC^{remin} (Methods for details).
318 The estimation of the biotic fraction of the DIC disequilibrium, DIC^{dis,bio}, is technically more complex as it is
319 based on a comparison between our default model and a model which lacks the impact of both biological carbon
320 pumps (‘biology’) on DIC and alkalinity, similar to Khatiwala et al., 2019 and Tjiputra et al., 2025. Deriving
321 DIC^{dis} from the differences of idealised tracers of preformed DIC and saturated DIC (Methods, Eq. 7), we quantify
322 DIC^{dis,bio} from the difference of the runs with and without biology (Methods, Eq. 8). This indirect approach is
323 needed since there is no meaningful definition of an abiotic DIC tracer in an Earth system model where
324 atmospheric CO₂ is affected by ocean biology, where atmospheric pCO₂ affects climate, and where climate in turn
325 affects ocean circulation and ocean biology.

326

327 In the following we evaluate AOUs converted to carbon units (the ‘AOU approximation’) against the sum DIC^{remin}
328 + DIC^{dis,bio}. We estimate a preindustrial global value of DIC^{dis,bio} of 520 Pg C and a global inventory of DIC^{remin}
329 of 1290 Pg C (Fig. 1b; Tab. S1). The sum of DIC^{remin} and DIC^{dis,bio} (1810 Pg C) suggests that the AOU-
330 approximation (1562 Pg C) is a modest underestimate of the preindustrial carbon attributable to the soft tissue
331 pump, i.e. by about 15% smaller than DIC^{remin} + DIC^{dis,bio} (Fig. 1b; Tab. S1).

332



333

334 **Fig. 3: AOU robustly estimates global inventories of TOU+O₂^{dis,bio}.** (a) AOU and TOU+O₂^{dis,bio} inventories (Pmol O₂)
 335 from model experiments conducted with variants of our UVic model which have been run to steady state (6000 model
 336 years) with either modified mixing and AMOC (and identical biogeochemical parameters) or identical physical
 337 parameters but differing particle flux attenuation. Thick dashed line is the 1:1 line and thin dashed lines represent the
 338 ±10% space around the 1:1 line. Data are from Frenger et al. 2024. (b) Changes in global inventories of AOU and
 339 TOU+O₂^{dis,bio} in RCP 8.5 CO₂-emission forced experiments carried out with the model variants used in (a). The change
 340 of global inventories by year 2100 relative to the preindustrial initial state is shown. (c) Changes in global inventories
 341 of AOU and TOU+O₂^{dis,bio} from model experiments with our default model variant forced with a suit of CO₂ and climate
 342 reversibility forcings (Koeve et al., 2024). The difference of inventories between yr 500 and the initial start year is
 343 shown. Compare Fig. S6 for transient atmospheric temperatures (ΔSAT, °C) and transient overturning (ΔAMOC, Sv)
 344 in model experiments explored in (c).



345 Turning to conditions of a changing climate, we have to consider that, in contrast to atmospheric O₂, the
346 atmospheric CO₂-boundary condition also changes considerably. This will affect the extent that reemerging
347 respiration CO₂ will outgas to the atmosphere and might make the carbon equivalent of AOU differ from
348 DIC^{remin}+DIC^{dis,bio}, an aspect that we will test in the following. Indeed, considering the change in the equilibration
349 of carbon based on our estimate of Δ DIC^{dis,bio} together with the change in the DIC^{remin} model tracer (Fig. 2b),
350 suggests that the Δ AOU-approximation is not a satisfying estimate, with an error of at least 40% compared with
351 Δ DIC^{remin} + Δ DIC^{dis,bio}. Moreover, during the first 100 years the AOU approximation appears to be unreliable.
352 Since, in our constant stoichiometry model, Δ DIC^{remin} and Δ TOU*RC:CO₂ agree to within a few percent (Fig. S7)
353 we urge to understand what drives Δ DIC^{dis,bio}. Specifically, we need to quantify the component of Δ DIC^{dis,bio} which
354 is associated with climate change, similar to that Δ O₂^{dis,bio} is affected by climate change, and the component which
355 is a mere response to the changing atmospheric CO₂-boundary condition. This needs another technical step: We
356 explore the behaviour of DIC^{dis,bio} in our default “fully coupled” simulation (COU*) and an additional simulation,
357 namely a merely “biogeochemically coupled” model experiment (BGC*) (Fig. 2c). The combination of fully
358 coupled and biogeochemically-only coupled experiments is a standard approach in Earth system modelling to
359 distinguish carbon-concentration feedbacks and carbon-climate feedbacks on atmospheric CO₂ (e.g., Arora et al,
360 2020). BGC* experiments “feel” CO₂ emissions like the default (COU*) model does, but the resultant climate
361 change is suppressed (technically the atmospheric CO₂ increase is neglected as radiative forcing in our model).
362 This means that there are no climate feedbacks in BGC* simulations, and the change in DIC reflects purely
363 “carbon-concentration effects”, in particular the marine uptake of anthropogenic CO₂ (C^{anth}). We adopt this
364 approach here, and obtain, by difference of the two experimental set ups, “ Δ DIC^{dis,bio,COU*-BGC*}”, the evolution of
365 Δ DIC^{dis,bio} under changing ocean circulation. Δ DIC^{dis,bio,COU*-BGC*} intentionally disregards the physico-chemical
366 effect of increasing atmospheric CO₂ on Δ DIC^{dis,bio}, Δ DIC^{dis,bio,BGC*}.
367
368 We find that over the entire experiment, Δ DIC^{dis,bio} is dominated by the effect of a changing atmospheric pCO₂-
369 boundary condition under constant climate (BGC*). Under a constant climate, circulation, sea ice, surface ocean
370 productivity and particle export (Fig. S8), as well as DIC^{remin} (Fig. S7, dashed lines) are in steady-state and do
371 not change over time. The change of DIC^{dis,bio} in this experiment can neither be related to biology itself and its
372 impact on carbon storage (‘gain side’ effects on C^{soft}, Frenger et al., 2024), nor to the circulation and ice cover
373 which could also affect storage attributable to the soft tissue pump if changed (‘loss side’ effects on C^{soft}, Frenger
374 et al., 2024), as either remain unchanged. Instead, the change in DIC^{dis,bio} in the BGC*-experiment is a response
375 to the transient increase of atmospheric pCO₂ (Fig. S8b), hence rather related to the physical-chemical invasion
376 of C^{anth}. Since oxygen does not have a respective (O₂^{anth}) effect, an AOU based estimate of C^{soft} is blind against
377 the C^{anth}-effect. In contrast, the difference of COU* and BGC* experiments of DIC^{dis,bio} reflects climate change
378 impacts such as changes in sea ice cover, circulation and biology on DIC^{dis,bio}.
379
380 It is a philosophical question if one wants to consider the BGC-effect or not. In most cases, however, like
381 observations from the ocean, and most climate climate models, it is either impossible or at least practically
382 difficult, demanding no-biology model setups and costly model spinup, to do so. Getting back to our motivation
383 to assess how well we can estimate effects of changes of the soft tissue pump based on AOU, in conclusion, we



384 find that the sum of our tracer based estimate of C^{soft} and $\Delta DIC^{dis,bio, COU-BGC^*}$ is larger than the AOU-approximation
385 on average by about 25%.
386

387 **4 Conclusion**

388 The computation of AOU is a pragmatic method which allows quantifying the O_2 debt stemming from organic
389 matter degradation in the ocean and its carbon equivalent. This method can be applied to available historical
390 observations, like global ocean data basis (Garcia et al., 2024), upcoming sensor based observations with
391 potentially high temporal and regional coverage, like those from the BGC-Argo program (Sharp et al., 2023), and
392 output from basically any ocean model that includes marine biogeochemistry (Wilson et al., 2022). As such it
393 provides a powerful tool to evaluate models, observe the signal of change in the real ocean and quantify the
394 contribution of carbon attributable to the soft tissue pump to the marine carbon sink under various potential futures
395 (Koeve et al., 2020; 2024; Wilson et al., 2022; Frenger et al., 2024).
396

397 This advantage comes with the need to state inherent assumptions of the AOU approach, understand how we can
398 interpret it, and the need of quantifying related uncertainties. As shown above, the AOU method includes
399 contributions in particular from an undersaturation of surface ocean waters with respect to atmospheric O_2 .
400 Hence, it overestimates the O_2 debt due to accumulated respiration of organic matter since last contact with the
401 atmosphere (so called ‘true’ oxygen utilisation; Ito et al., 2004; Duteil et al., 2013). Given that, as shown above,
402 most of this overestimate is attributable to the *biotic* O_2 disequilibrium, i.e., that the O_2 debt of upwelled waters,
403 stemming from former organic matter degradation, tends to not fully get replenished with atmospheric O_2 before
404 re-subduction of waters, AOU provides a reasonable estimate of the *total* accumulated O_2 debt due to oxic organic
405 matter degradation, which globally is correct to within about 10% error for most of the preindustrial state estimate
406 and the transient climate change scenarios studied here.
407

408 The fraction of total DIC attributable of the soft tissue pump has been estimated to about 1300 ± 230 Pg C (Carter
409 et al., 2021; Nowicki et al., 2022), or about 3.5% of the total DIC inventory (37,300 Pg C; DeVries 2022). By
410 definition of the chosen approaches in the respective studies, the estimate of 1300 ± 230 Pg C is a state estimate
411 of the DIC attributable to the marine soft tissue pumps accumulated *since last contact with the atmosphere*. The
412 respective DIC^{remin} inventory state estimate in our model, within uncertainty, is the same (1290 Pg C). In the real
413 ocean, C^{soft} can not be distinguished by chemical analysis from the large background inventory of DIC, but AOU
414 provides this insight/information. Given that, as outlined above, AOU considers the accumulated O_2 debt due to
415 oxic organic matter degradation, this is the case also for the AOU-based estimate of respired carbon: it includes
416 the effect from incomplete equilibration of re-surfacing old waters that are enriched with carbon. We here assess
417 technical uncertainties of using AOU to estimate remineralized carbon and find that for the preindustrial state
418 estimate the AOU-approximation (1562 Pg C) is an about 15% underestimate of the sum of the DIC^{remin} and
419 $DIC^{dis,bio}$.
420



421 For the climate change transient we find that ΔAOU underestimates the disequilibrium ‘corrected’ change in C^{soft}
422 ($\text{DIC}^{\text{remin}} + \text{DIC}^{\text{dis,bio,COU*}-\text{BGC}}$) by 25%. An additional aspect, that we do not have for O_2 , is that atmospheric CO_2
423 changes (increases; while atmospheric O_2 remains quasi-constant). The transient increase of atmospheric CO_2
424 itself, everything else unchanged, brings CO_2 -oversaturated surface ocean waters closer to equilibration. Since
425 this applies to the experiments with and without biology alike, it reduces the biotic component of incomplete
426 equilibration ($\text{DIC}^{\text{dis,bio}}$) which is computed by the difference of these experiments.
427 Importantly, quantifying $\text{DIC}^{\text{dis,bio}}$ requires additional no-biology model variants, spinups and transient
428 experiments and therefore is computationally very demanding.
429
430 Quantifying explicitly the climate change effect on $\text{DIC}^{\text{dis,bio}}$ is even more demanding, requiring fully coupled and
431 biogeochemically coupled transient experiments carried out with both model variants. Assessing $\text{DIC}^{\text{dis,bio, COU*}-$
432 BGC^* in climate models is hence technically very challenging and costly. Said that, we suggest that ΔAOU provides,
433 while not perfect, a quite satisfying metric for the change of marine excess carbon from the soft tissue pump under
434 anthropogenic climate change.

435 **Code and data availability**

436 Model code, forcing files and output are available from GEOMAR at the following data archives:
437 <https://hdl.handle.net/20.500.12085/209f14f8-4c41-4e93-abe4-65a0af271fa6>;
438 <https://hdl.handle.net/20.500.12085/74a83d93-c755-44c1-a615-2cfa4197f016> and
439 <https://hdl.handle.net/20.500.12085/959a266e-d785-4d57-87bb-103b28d2bb25>.
440

441 **Author contributions**

442 W.K. and I.F. designed the research
443 W.K. performed the model experiments
444 W.K. analysed model output
445 W.K. and I.F. wrote the manuscript

446 **Competing interest**

447 The authors declare that they have no conflict of interest

448 **Acknowledgements**

449 The authors like to thank colleagues from the Biogeochemical Modelling (BM) at GEOMAR, in particular
450 Haichao Guo, Ying Cui, and Dunuhinge Amawi Nimesha Silva and members of the Carbon in the Anthropocene
451 BM working group. We acknowledge funding by the European Union (ERC, OSTIA, 101116545) (I.F.). This
452 work is a contribution to the GEOMAR POF IV program ‘Changing Earth – Sustaining our Future, Topic 6.3:
453 The Future Biological Carbon Pump’.



454 **References**

455 Arora, V. K., Katavouta, A., Williams, R. G., Jones, C. D., Brovkin, V., Friedlingstein, P., Schwinger, J., Bopp, L., Boucher, O., Cadule, P., Chamberlain, M. A., Christian, J. R., Delire, C., Fisher, R. A., Hajima, T., Ilyina, T., Joetzjer, E., Kawamiya, M., Koven, C. D., Krasting, J. P., Law, R. M., Lawrence, D. M., Lenton, A., Lindsay, K., Pongratz, J., Raddatz, T., Séférian, R., Tachiiri, K., Tjiputra, J. F., Wiltshire, A., Wu, T., and Ziehn, T.: Carbon-concentration and carbon-climate feedbacks in CMIP6 models and their comparison to CMIP5 models, *Biogeosciences*, 17, 4173–4222, <https://doi.org/10.5194/bg-17-4173-2020>, 2020.

461 Bernardello, R., Marinov, I., Palter, J. B., Sarmiento, J. L., Galbraith, E. D., and Slater, R. D.: Response of the
462 Ocean Natural Carbon Storage to Projected Twenty-First-Century Climate Change, *Journal of Climate*, 27, 2033–
463 2053, <https://doi.org/10.1175/JCLI-D-13-00343.1>, 2014.

464 Carter, B. R., Feely, R. A., Lauvset, S. K., Olsen, A., DeVries, T., and Sonnerup, R.: Preformed Properties for
465 Marine Organic Matter and Carbonate Mineral Cycling Quantification, *Global Biogeochemical Cycles*, 35,
466 e2020GB006623, <https://doi.org/10.1029/2020GB006623>, 2021.

467 DeVries, T.: The Ocean Carbon Cycle, *Annu. Rev. Environ. Resour.*, 47, 317–341,
468 <https://doi.org/10.1146/annurev-environ-120920-111307>, 2022.

469 Dietze, H. and Oschlies, A.: Modeling abiotic production of apparent oxygen utilisation in the oligotrophic
470 subtropical North Atlantic, *Ocean Dynamics*, 55, 28–33, <https://doi.org/10.1007/s10236-005-0109-z>, 2005.

471 Doval, M. D. and Hansell, D. A.: Organic carbon and apparent oxygen utilization in the western South Pacific
472 and the central Indian Oceans, *Marine Chemistry*, 68, 249–264, [https://doi.org/10.1016/S0304-4203\(99\)00081-X](https://doi.org/10.1016/S0304-4203(99)00081-X), 2000.

474 Duteil, O. and Oschlies, A.: Sensitivity of simulated extent and future evolution of marine suboxia to mixing
475 intensity, *Geophysical Research Letters*, 38, <https://doi.org/10.1029/2011GL046877>, 2011.

476 Duteil, O., Koeve, W., Oschlies, A., Bianchi, D., Galbraith, E., Kriest, I., and Matear, R.: A novel estimate of
477 ocean oxygen utilisation points to a reduced rate of respiration in the ocean interior, *Biogeosciences*, 10, 7723–
478 7738, <https://doi.org/10.5194/bg-10-7723-2013>, 2013.

479 Eby, M., Weaver, A. J., Alexander, K., Zickfeld, K., Abe-Ouchi, A., Cimatoribus, A. A., Crespin, E., Drijfhout,
480 S. S., Edwards, N. R., Eliseev, A. V., Feulner, G., Fichefet, T., Forest, C. E., Goosse, H., Holden, P. B., Joos, F.,
481 Kawamiya, M., Kicklighter, D., Kienert, H., Matsumoto, K., Mokhov, I. I., Monier, E., Olsen, S. M., Pedersen, J.
482 O. P., Perrette, M., Philippon-Berthier, G., Ridgwell, A., Schlosser, A., Schneider Von Deimling, T., Shaffer, G.,
483 Smith, R. S., Spahni, R., Sokolov, A. P., Steinacher, M., Tachiiri, K., Tokos, K., Yoshimori, M., Zeng, N., and
484 Zhao, F.: Historical and idealized climate model experiments: an intercomparison of Earth system models of
485 intermediate complexity, *Clim. Past*, 9, 1111–1140, <https://doi.org/10.5194/cp-9-1111-2013>, 2013.

486 Emerson, S., Mecking, S., and Abell, J.: The biological pump in the subtropical North Pacific Ocean: Nutrient
487 sources, Redfield ratios, and recent changes, *Glob. Biogeochem. Cycle*, 15, 535–554,
488 <https://doi.org/10.1029/2000GB001320>, 2001.

489 Frenger, I., Landolfi, A., Karin Kvale, Somes, C. J., Oschlies, A., Yao, W., and Koeve, W.: Misconceptions of
490 the marine biological carbon pump in a changing climate: Thinking outside the “export” box, *Global Change
491 Biology*, 30, e17124, <https://doi.org/10.1111/gcb.17124>, 2024.

492 Garcia, H. E. and Gordon, L. I.: Oxygen solubility in seawater: Better fitting equations, *Limnology and
493 Oceanography*, 37, 1307–1312, <https://doi.org/10.4319/lo.1992.37.6.1307>, 1992.



494 Garcia, H. E., Locarnini, R. A., Boyer, T. P., Antonov, J. I., Baranova, O. K., Reagan, J. R., and Johnson, D. R.:
495 World Ocean Atlas 2013, Volume 3: Dissolved Oxygen, Apparent Oxygen Utilization, and Oxygen Saturation.
496 Technical Ed.; NOAA Atlas NESDIS 75, 27 pp., 2014.

497 Garcia, H.E., Z. Wang, C. Bouchard, S.L. Cross, C.R. Paver, J.R. Reagan, T.P. Boyer, R.A. Locarnini, A.V.
498 Mishonov, O. Baranova, D. Seidov, and D. Dukhovskoy: Oxygen, World Ocean Atlas 2023, Volume 3: Dissolved
499 Oxygen, Apparent Oxygen Utilization, and Oxygen Saturation., 2024.

500 Gordon, A. L. and Huber, B. A.: Southern ocean winter mixed layer, *J. Geophys. Res.*, 95, 11655–11672,
501 <https://doi.org/10.1029/JC095iC07p11655>, 1990.

502 Gruber, N., Sarmiento, J. L., and Stocker, T. F.: An improved method for detecting anthropogenic CO₂ in the
503 oceans, *Global Biogeochemical Cycles*, 10, 809–837, <https://doi.org/10.1029/96GB01608>, 1996.

504 Gutiérrez-Loza, L., Nilsson, E., Wallin, M. B., Sahlée, E., and Rutgersson, A.: On physical mechanisms enhancing
505 air–sea CO₂ exchange, *Biogeosciences*, 19, 5645–5665, <https://doi.org/10.5194/bg-19-5645-2022>, 2022.

506 Ito, T. and Follows, M. J.: Preformed phosphate, soft tissue pump and atmospheric CO₂, *J. Mar. Res.*, 63, 813–
507 839, 2005.

508 Ito, T., Follows, M. J., and Boyle, E. A.: Is AOU a good measure of respiration in the oceans?, *Geophysical
509 Research Letters*, 31, 2004GL020900, <https://doi.org/10.1029/2004GL020900>, 2004.

510 Ito, T., Minobe, S., Long, M. C., and Deutsch, C.: Upper ocean O₂ trends: 1958–2015, *Geophys. Res. Lett.*, 44,
511 4214–4223, <https://doi.org/10.1002/2017GL073613>, 2017.

512 Jones, C. D., Frölicher, T. L., Koven, C., MacDougall, A. H., Matthews, H. D., Zickfeld, K., Rogelj, J., Tokarska,
513 K. B., Gillett, N. P., Ilyina, T., Meinshausen, M., Mengis, N., Séférian, R., Eby, M., and Burger, F. A.: The Zero
514 Emissions Commitment Model Intercomparison Project (ZECMIP) contribution to C4MIP: quantifying
515 committed climate changes following zero carbon emissions, *Geoscientific Model Development*, 12, 4375–4385,
516 <https://doi.org/10.5194/gmd-12-4375-2019>, 2019.

517 Keeling, R. F., Körtzinger, A., and Gruber, N.: Ocean Deoxygenation in a Warming World, *Annu. Rev. Mar. Sci.*,
518 2, 199–229, <https://doi.org/10.1146/annurev.marine.010908.163855>, 2010.

519 Keller, D. P., Oschlies, A., and Eby, M.: A new marine ecosystem model for the University of Victoria Earth
520 System Climate Model, *Geosci. Model Dev.*, 5, 1195–1220, <https://doi.org/10.5194/gmd-5-1195-2012>, 2012.

521 Khatiwala, S., Schmittner, A., and Muglia, J.: Air-sea disequilibrium enhances ocean carbon storage during glacial
522 periods, *Sci. Adv.*, 5, eaaw4981, <https://doi.org/10.1126/sciadv.aaw4981>, 2019.

523 Koeve, W., Kähler, P., and Oschlies, A.: Does Export Production Measure Transient Changes of the Biological
524 Carbon Pump's Feedback to the Atmosphere Under Global Warming?, *Geophysical Research Letters*, 47,
525 e2020GL089928, <https://doi.org/10.1029/2020GL089928>, 2020.

526 Koeve, W., Landolfi, A., Oschlies, A., and Frenger, I.: Marine carbon sink dominated by biological pump after
527 temperature overshoot, *Nat. Geosci.*, 17, 1093–1099, <https://doi.org/10.1038/s41561-024-01541-y>, 2024.

528 Körtzinger, A., Hedges, J. I., and Quay, P. D.: Redfield ratios revisited: Removing the biasing effect of
529 anthropogenic CO₂, *Limnology and Oceanography*, 46, 964–970, <https://doi.org/10.4319/lo.2001.46.4.00964>,
530 2001.

531 Körtzinger, A., Schimanski, J., Send, U., and Wallace, D.: The ocean takes a deep breath, *Science*, 306, 1337–
532 1337, <https://doi.org/10.1126/science.1102557>, 2004.



533 Mackay, N. and Watson, A.: Winter Air-Sea CO₂ Fluxes Constructed From Summer Observations of the Polar
534 Southern Ocean Suggest Weak Outgassing, *Journal of Geophysical Research: Oceans*, 126, e2020JC016600,
535 <https://doi.org/10.1029/2020JC016600>, 2021.

536 Nowicki, M., DeVries, T., and Siegel, D. A.: Quantifying the Carbon Export and Sequestration Pathways of the
537 Ocean's Biological Carbon Pump, *Global Biogeochemical Cycles*, 36, e2021GB007083,
538 <https://doi.org/10.1029/2021GB007083>, 2022.

539 Ogura, N.: The relation between dissolved organic carbon and apparent oxygen utilization in the Western North
540 Pacific, *Deep Sea Research and Oceanographic Abstracts*, 17, 221–231, [https://doi.org/10.1016/0011-7471\(70\)90016-1](https://doi.org/10.1016/0011-7471(70)90016-1), 1970.

541 Oschlies, A., Koeve, W., Landolfi, A., and Kähler, P.: Loss of fixed nitrogen causes net oxygen gain in a warmer
542 future ocean, *Nat Commun*, 10, 2805, <https://doi.org/10.1038/s41467-019-10813-w>, 2019.

543 Redfield, A.: The processes determining the concentration of oxygen, phosphate and other organic derivatives
544 within the depths of the Atlantic ocean, *Pap. Phys. Oceanogr. Meteorol.*, 9, 1–22, 1942.

545 Redfield, A. C.: On the proportions of organic derivatives in sea water and their relation to the composition of
546 plankton, in: *James Johnstone memorial volume*, 176–192, 1934.

547 Salter, M. E., Upstill-Goddard, R. C., Nightingale, P. D., Archer, S. D., Blomquist, B., Ho, D. T., Huebert, B.,
548 Schlosser, P., and Yang, M.: Impact of an artificial surfactant release on air-sea gas fluxes during Deep Ocean
549 Gas Exchange Experiment II, *Journal of Geophysical Research: Oceans*, 116,
550 <https://doi.org/10.1029/2011JC007023>, 2011.

551 Sarmiento, J. L. and Gruber, N.: *Ocean Biogeochemical Dynamics*, Princeton University Press,
552 <https://doi.org/10.2307/j.ctt3fgxqx>, 2006.

553 Schmidtko, S., Stramma, L., and Visbeck, M.: Decline in global oceanic oxygen content during the past five
554 decades, *Nature*, 542, 335–+, <https://doi.org/10.1038/nature21399>, 2017.

555 Schwinger, J. and Tjiputra, J.: Ocean Carbon Cycle Feedbacks Under Negative Emissions, *Geophysical Research
556 Letters*, 45, 5062–5070, <https://doi.org/10.1029/2018GL077790>, 2018.

557 Sharp, J. D., Fassbender, A. J., Carter, B. R., Johnson, G. C., Schultz, C., and Dunne, J. P.: GOBAI-O₂: temporally
558 and spatially resolved fields of ocean interior dissolved oxygen over nearly 2 decades, *Earth System Science Data*,
559 15, 4481–4518, <https://doi.org/10.5194/essd-15-4481-2023>, 2023.

560 Takano, Y., Ito, T., and Deutsch, C.: Projected Centennial Oxygen Trends and Their Attribution to Distinct Ocean
561 Climate Forcings, *Glob. Biogeochem. Cycle*, 32, 1329–1349, <https://doi.org/10.1029/2018GB005939>, 2018.

562 Tanioka, T. and Matsumoto, K.: Stability of Marine Organic Matter Respiration Stoichiometry, *Geophysical
563 Research Letters*, 47, e2019GL085564, <https://doi.org/10.1029/2019GL085564>, 2020.

564 Tjiputra, J. F., Couespel, D., and Sanders, R.: Marine ecosystem role in setting up preindustrial and future climate,
565 *Nat Commun*, 16, 2206, <https://doi.org/10.1038/s41467-025-57371-y>, 2025.

566 Volk, T. and Hoffert, M. I.: Ocean carbon pumps, analysis of relative strengths and efficiencies in ocean-driven
567 atmosphere CO₂ changes, in: *The carbon cycle and atmospheric CO₂: natural variations archean to present*, vol.
568 32, AGU, Washington, D.C., 99–110, 1985.

569 Wanninkhof, R.: Relationship between wind speed and gas exchange over the ocean revisited, *Limnology &
570 Ocean Methods*, 12, 351–362, <https://doi.org/10.4319/lom.2014.12.351>, 2014.

571



572 Weaver, A. J., Eby, M., Wiebe, E. C., Bitz, C. M., Duffy, P. B., Ewen, T. L., Fanning, A. F., Holland, M. M.,
573 MacFadyen, A., Matthews, H. D., Meissner, K. J., Saenko, O., Schmittner, A., Wang, H., and Yoshimori, M.: The
574 UVic earth system climate model: Model description, climatology, and applications to past, present and future
575 climates, *Atmosphere-Ocean*, 39, 361–428, <https://doi.org/10.1080/07055900.2001.9649686>, 2001.

576 Wilson, J. D., Andrews, O., Katavouta, A., De Melo Viríssimo, F., Death, R. M., Adloff, M., Baker, C. A.,
577 Blackledge, B., Goldsworth, F. W., Kennedy-Asser, A. T., Liu, Q., Sieradzan, K. R., Vosper, E., and Ying, R.:
578 The biological carbon pump in CMIP6 models: 21st century trends and uncertainties, *Proc. Natl. Acad. Sci.*
579 U.S.A.

580 e119, e2204369119, <https://doi.org/10.1073/pnas.2204369119>, 2022.

581 Wolf, M. K., Hamme, R. C., Gilbert, D., Yashayaev, I., and Thierry, V.: Oxygen Saturation Surrounding Deep
582 Water Formation Events in the Labrador Sea From Argo-O2 Data, *Global Biogeochemical Cycles*, 32, 635–653,
<https://doi.org/10.1002/2017GB005829>, 2018.